IOSR Journal of Mechanical and Civil Engineering (IOSR-JMCE)
e-ISSN: 2278-1684,p-ISSN: 2320-334X, Volume 15, Issue 1 Ver. IV (Jan. - Feb. 2018), PP 33-43
www.iosrjournals.org

Simulation of Physiological Non-Newtonian Blood Flow through 3-D Geometry of Carotid Artery with Stenosis

Khairuzzaman Mamun[1], Most. Nasrin Akhter[2], and Ken-ichi Funazaki[1]
1(Mechanical Engineering Department, Iwate University, Morioka, Iwate, Japan)
2(Department of Mathematics, Dhaka University of Engineering and Technology, Gazipur-1700, Bangladesh)
Corresponding Author: Khairuzzaman Mamun

Abstract: *A numerical simulation has been performed to investigate blood flow behavior of three dimensional idealized carotid arteries. Non-Newtonian flow has been taken for the simulation. The wall of the vessel is considered to be rigid. Physiological and parabolic velocity profile has been imposed for inlet boundary condition. Reynolds number at the inlet has been ranged approximately from 86 to 966 for the investigation. Low Reynolds number k-w model has been used as governing equation. The investigations have been carried out to characterize the flow behavior of blood. The numerical results have been presented in terms of wall shear stress distributions, streamlines contours and axial velocity contours. However, highest wall shear stress has been observed in the bifurcation area. Unexpectedly, transient or unstable flow has created flow disturbance regions in the arteries. Moreover, the disturbance of flow has risen as the severity of stenosis in the artery has been increased.*

Keywords *- Atherosclerosis, Carotid artery, Physiological flow, Stenosis, Viscoelastic fluid*

Date of Submission: 09-02-2018 Date of acceptance: 24-02-2018

I. Introduction

The carotid arteries are located on both side of the neck, the blood vessels that carry oxygenated blood to the head, brain and face. Actually, they supply essential oxygenated blood to the large front part of the brain which controls thought, speech, personality as well as our sensory (our ability to feel) and motor (our ability to move) functions. Besides, the brain survives on a continuous supply of oxygen and glucose carried by blood through it. Thus, Carotid artery disease such as stenosis in the carotid artery can cause cerebral disturbance. However, stenosis in the artery is an abnormal constriction of the artery. Generally, arteries are strong and flexible blood vessels that can expand and contract with heartbeats. They contain endothelium (a thin layer of cells) that keeps the artery smooth and allows blood to flow easily. However, the endothelium becomes damaged by accumulating Lower Density Lipoprotein (LDL cholesterol) in the artery wall. On the other hand, the body sends macrophage white blood cells to clean up the cholesterol, but sometimes the cells get stuck there and gradually build up plaque with bad cholesterol (LDL cholesterol) at the affected site. Thus, the arterial wall loses its flexibility which decreases the area of artery which is called arterial stenosis.

The initial research on blood flow within stenosed arteries concentrated on experimental simulations. Smith [1] conducted extensive studies of steady flows through an axisymmetric stenosed artery using an analytical approach where he revealed that the resulting flow patterns were highly dependent on geometry of the stenosis and the overall Reynolds number of the flow. Another study investigated by Deshpande et al [2] depicted the finite difference scheme to solve the flow through an axisymmetric stenosis under steady flow and arrived at similar conclusions. An investigation by Young and Tsai [3] provided experimental analysis on steady flow through stenosed arteries with varying severity, stenosis length, axisymmetric and asymmetric conditions, and with a range of Reynolds numbers from laminar to turbulent flows. It was found that all these factors contributed significantly to the flow behavior. As expected, low fluid Reynolds number, smooth stenosis transitions and low degrees of severity tended to have little effect on the flow. Later studies have shown that in order to approach realistic conditions, it is not possible to neglect the time-varying nature of the flow within the arteries. Other studies have thus included transient conditions into their simulations in order to take into account this flow behavior. Imaeda and Goodman [4] performed simulations on non-linear pulsatile blood flow in large arteries to determine the stability of the code and model used as well as to provide a proper representation of higher-frequency components. In addition, this code attempted to account for the viscoelastic properties of the wall in terms of wall motion and the effect on the fluid. Misra and Chakravaty [5] also performed simulations of arteries incorporating stenosis and assuming blood as a Newtonian fluid. The effect of artery wall response was also incorporated into the simulation and fluid harmonic waves were studied. Young and Tsai [6] further extended their previous experiment to include oscillation flows with the aim of deriving an equation to describe

the pressure drop across the tube. The results indicated that oscillation tended to produce flow, which was effectively different from steady state conditions, in some cases increasing the stability of the flow. Taking into account the fluid momentum can effectively change the flow recirculation characteristics, such as during the deceleration phase, a low-pressure difference between the inlet and the outlet will occur, which increases the recirculation effects. The comparison of stenosed flow behavior with the normal one can provide the proper understanding of underlying mechanism behind the development of atherosclerosis. The flow turns to be abnormal in the reduced cross sectional area of the artery stated by Kader and Shenory [7]. The flow behavior in the stenosed artery is quite different in comparison to the normal one. Stress and resistance to flow is much higher in stenosed artery. Chua and Shread [8] found that the flow through the constricted tube is characterized by high velocity jet generated at constricted region. Kader and Shenory [7] found the results from numerical simulation which demonstrated that velocity and stenotic jet length increases in increasing the severity of stenosis. Their results also demonstrate that the 3D stenotic CFD model is capable of predicting the changes in flow behavior for increased severity of stenosis. Young et al. [9] studied the wall shear stress and pressure gradient in the stenosis and evaluated the cause of plaque rupture. Stenosis located in the carotid arteries is not only prevalent, but also represents a significant risk for clinical cerebrovascular events. The carotid artery with stenosis is the most common reason for stroke. Carotid arteries are responsible for 10 – 30% of all strokes, estimated by Khader and Shenoy [7]. At the stenosed carotid artery, flow first goes through a stenotic flow constriction then immediately encounters an asymmetric bifurcating junction. The bifurcation imposes a flow division that affects the boundary layers along both the inside and outside bends. Chua and Shread [8] investigated that stenoses, bifurcations, and surface roughness are closely associated with flow disturbances and complex flow. Even the normal and healthy vessel with bends, bifurcations as well as pulsatile flow of the cardiac cycle introduces secondary flows and oscillating shear stresses. Thus, stenosis admits more complications particularly where arterial disease is severe according to Stroud et al [10]. Besides, tortuous, irregular vessel surfaces are likely to further contribute to flow disturbances, studied by Chua and Shread [8].

A highly disturbed flow may be led by a severe stenosis. This disturbed flow may either remain laminar or may undergo transition to turbulent flow, depending on the stenosis. However, turbulence presents some abnormalities in the blood flow circulation and is linked to various vascular disorders, according to Boughner and Roach [11]; Cassanova and Giddens [12]. Thus, the development of turbulent flow has important clinical consequences. Besides, it may also lead to significant losses in pressure and abnormally high shear stresses, which may result in hemolysis and the activation of platelets. Roach [13] has recognized that turbulence in stenotic regions is very much possible. Therefore several numerous experiments have been conducted to study the existence of turbulence in blood flow through arteries in animals by Giddens et al. [14], with stenosis by Clark [15] and in humans by Strandness et al [16].From these studies, they made conclusion that transitional flow or turbulence can be expected distal to the constriction. Moreover, Yongchareon and Young [17]; Jones [18] found very important result from their Experimental studies that the critical Reynolds number at which flow becomes transitional or turbulent in a stenosis is a function of its severity, being 1,100 for a 50% stenosis and 400 for a 75% stenosis.

The assumption of Newtonian behavior of blood is acceptable for flow in large arteries, and of high Reynolds number and high shear rate stated by Rabby et al [19]. In case of pulsatile blood flow there are some moments (like diastole, early systole) when blood flow has low Reynolds number. Moreover, in various arteries there are some locations (such as pre-stenotic region) where blood flow has low Reynolds number or low shear rate. However, it has been demonstrated that assigning Newtonian behavior to blood is only valid when it has shear rates in excess of 100s-1, which tends to occur in larger arteries, according to Pedley [20]; Berger and Jou [21]. Therefore, in most cases, non-Newtonian blood models would provide a more accurate representation of blood flow behavior within the arteries, particularly for stenosed conditions. It was also revealed that some diseased condition like severe myocardial infarction, cerebrovascular diseases and hypertension, blood exhibits remarkable Non-Newtonian properties by Chien [22]. According to Berger and Jou [21], if the shear rate is high, the blood behaves like a Newtonian fluid whose viscosity be 0.00345Pa·s. However, if the Reynolds number or shear rate of blood flow falls down due to various diseased conditions, its viscosity increases and blood exhibits Non-Newtonian property.

In the present study, we planned to simulate blood flow in carotid arteries with stenosis using the low-Reynolds number k-w turbulence model, according to Wilcox [24]. The Cross model has been implemented in the simulation to approximate the non-Newtonian flow. Numerical simulation of blood flow offers detailed flow patterns, such as wall shear stress distributions, which are very difficult to obtain experimentally. Thus, wall shear stress distributions, streamlines contours and axial velocity contours have been presented to analyze the flow characteristics.

II. Model Description

2.1. Geometry

Three idealized 3-D Carotid arteries have been used as geometry for this study, shown in figure 1. One healthy and two stenotic Carotid arteries (with different severities such as 65% and 85% stenosis) have been investigated where stenoses are located before the bifurcation of the arteries. The wall is considered to be rigid. These carotid arteries are modeled by using ANSYS Workbench. However, the model divided into three parts such as Common Carotid Artery (the zone just before the bifurcation), Internal Carotid artery (the right bifurcated part) and External Carotid Artery (left bifurcated part). The length (L) of the models is 72 mm. Moreover, the diameter of the inlet of the model, end of ICA and end of ECA are 6mm, 3.75 mm and 2.5 mm respectively. The flow field meshing information of different arteries has been presented in the Table 1.

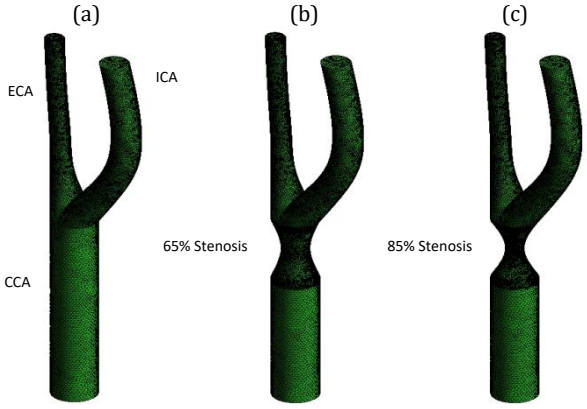

Fig. 1: (a) Healthy Carotid Artery, (b) 65% stenotic Carotid Artery and (C) 85% stenotic Carotid Artery.

Table 1: Number of nodes and elements of different arteries.

Meshing information	Healthy Carotid Artery	65% stenotic Carotid Artery	85% stenotic Carotid Artery
Number of Nodes	59131	83191	87855
Number of Elements	296480	421822	445970

2.2. Blood properties

Blood is taken as fluid where the density of the blood is 1050kg/m^3. Moreover, blood is considered Non-Newtonian fluid, so the viscosity of the blood is calculated from cross model. Malcolm M. Cross [25] proposed a shear rate dependent viscosity model called Cross model. The Cross model is defined by the following equation.

$$\mu = \mu_\infty + (\mu_0 - \mu_\infty)\left[1 + \left(\frac{|\dot{\gamma}|}{\gamma_c}\right)^m\right]^{-1}$$

Where, $\mu_0 = 0.0364 Pa.s$ is the usual molecular blood viscosity for zero shear rates, $\mu_\infty = 0.00345 Pa.s$when shear rates is high, $\gamma_c = 2.63\ s^{-1}$ is the reference shear rate, $\dot{\gamma}$ is the instantaneous shear rate, and m=1.45 is the constant.

III. Governing Equation And Boundary Condition

3.1. Governing equation

In the present study, we simulated our numerical modeling on blood flows with low Reynolds numbers ranging approximately from 86 to 966. In this range of Reynolds numbers, the viscous sub-layer is very much thick, so flow should be laminar theoretically. However, we used 85% constriction in a Carotid Artery for simulation, so blood passes through the throat and post stenotic region with high velocity. Naturally the Reynolds number will increase at the throat. Figure (2) presents the comparison of Re-Number variation with time at inlet and throat region of 85% stenotic Carotid Artery. The highest Reynolds number is about 3736 at the throat. Thus, the flow may undergo transition to turbulent for this condition.

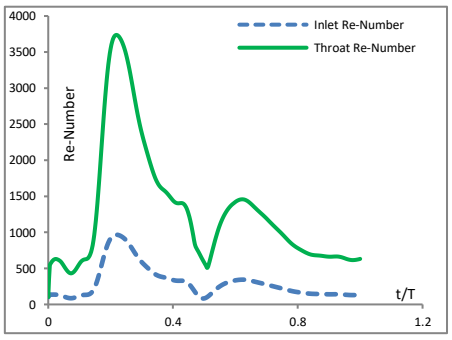

Fig. 2: Re-Number variation with time at 85% stenotic Carotid Artery.

Neither laminar flow modeling nor standard two-equation models are suitable for this kind of blood flow. We therefore chose the Wilcox low-Re k-w turbulence model for our simulation. However, the Navier-Stokes equations can be given by (1) and (2).

$$\frac{\partial u_i}{\partial x_i} = 0 \tag{1}$$

$$\frac{\partial u_i}{\partial t} + u_j \frac{\partial u_i}{\partial x_j} = -\frac{1}{\rho}\frac{\partial p}{\partial x_i} + \nu \frac{\partial^2 u_i}{\partial x_j \partial x_j} \tag{2}$$

Since each term of this equation is time averaged, the equation is referred to as a Reynolds averaged Navier-Stokes (RANS) equation. During this procedure, several additional unknown parameters appear which require additional equations to be introduced as turbulence models. The set of RANS equations are presented by the equations (3) and (4).

$$\frac{\partial \rho}{\partial t} + \frac{\partial (\rho u_i)}{\partial x} = 0 \tag{3}$$

$$\frac{\partial (\rho u_i)}{\partial t} + \frac{\partial (\rho u_i u_j)}{\partial x_j} = -\frac{\partial p}{\partial x_i} + \frac{\partial}{\partial x_j}\left[\mu\left(\frac{\partial u_i}{\partial x_j} + \frac{\partial u_j}{\partial x_i}\right)\right] + \frac{\partial}{\partial t}(-\rho\overline{u_i' u_j'}) \tag{4}$$

In this equation $(-\rho\overline{u_i' u_j'})$ is an additional term known as the Reynolds's stress tensor, which can be approximated by using Boussinesq's hypothesis, (5).

$$-\rho\overline{u_i' u_j'} = \mu_t\left(\frac{\partial u_i}{\partial x_j} + \frac{\partial u_j}{\partial x_i}\right) - \frac{2}{3}\rho k \delta_{ij} \tag{5}$$

The k equation -

$$\rho u_j \frac{\partial k}{\partial x_j} = \frac{\partial}{\partial x_j}\left[\left(\mu + \frac{\mu_t}{\sigma_k}\right)\frac{\partial k}{\partial x_j}\right] + G - \rho\omega k \tag{6}$$

The ω equation -

$$\rho u_j \frac{\partial \omega}{\partial x_j} = \frac{\partial}{\partial x_j}\left[\left(\mu + \frac{\mu_t}{\sigma_\omega}\right)\frac{\partial \omega}{\partial x_j}\right] + c_1 \frac{\omega}{k} G - c_2 \rho \omega^2 \tag{7}$$

Where turbulent viscosity

$\mu_t = c_\mu \rho \frac{k}{\omega}$ and the generation rate of turbulence kinetic energy

$$G = \mu_t\left(\frac{\partial u_i}{\partial x_j} + \frac{\partial u_j}{\partial x_i}\right)\frac{\partial u_i}{\partial x_j}$$

The values of the Wilcox model constants were:

$c_1 = 0.555,\ c_2 = 0.8333,\ c_\mu = 0.09,\ \sigma_k = 2$ and $\sigma_\omega = 2$.

3.2. Boundary condition

Since the blood flow through arterial stenosis is an unsteady phenomenon and the blood flow to be fully developed at inlet region, physiological parabolic velocity profile has been imposed for inlet boundary condition. For this purpose one user defined function has been written in C++ programming language to demonstrate the unsteady parabolic nature of velocity profile using the relationship given in the equation (8) and (9).

$$u_x = u\left(1 - \frac{y^2 + z^2}{\text{radius}^2}\right) \tag{8}$$

Where, $u = \sum_{n=0}^{n=16}(A_n \cos(ft) + B_n \sin(ft))$ (9)

Where, A_n and B_n are the coefficients, shown in the table 2 according to Mamun et al. [26].

Table 2: Harmonic coefficients for pulsatile waveform shown in figure 2(a).

n	A_n	B_n	n	A_n	B_n	n	A_n	B_n
0	0.166667	0	6	0.01735	0.01915	12	-0.00341	0.005463
1	-0.03773	0.0985	7	-0.00648	0.002095	13	-0.00194	0.000341
2	-0.10305	0.012057	8	-0.01023	-0.0078	14	-0.00312	-0.00017
3	0.007745	-0.06763	9	0.008628	-0.00663	15	0.000157	-0.00299
4	0.025917	-0.02732	10	0.002267	0.001817	16	0.001531	0.000226
5	0.037317	0.024517	11	0.005723	0.003352			

In this study Reynolds number varies from 86 to 966. Since cardiac pulse cycle is 0.82sec, f is found from the equation (10).

$$f = \frac{2\pi}{0.82} = 7.66 \text{ rad/sec} \tag{10}$$

Figure 3(a) shows physiological waveform and 3(b) and 3(c) depict the graph and contour parabolic inlet velocity profile. The hemodynamic parameters were measured at four different time instants during the cardiac cycle. These four time instants represent critical flow rate phases in the cardiac cycle. In figure 3(a), a, b, c and d represent the positions of early systole (0.0574 sec), peak systole (0.1804 sec), early diastole (0.41 sec) and diastole (0.5125 sec) respectively. However, early systole is the condition when the blood starts its journey

of flowing through the arteries. Actually, it is the beginning time of rising arterial pressure. Besides, peak systole happens when the arterial pressure is highest. On the other hand, when arteries are relaxed and allow for the new blood to flow, it is known as diastole.

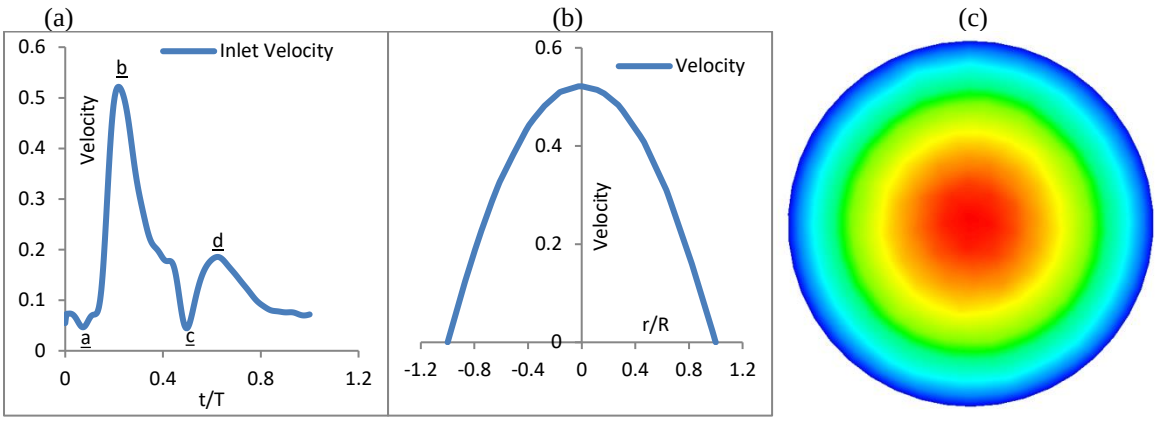

Fig. 3: (a) Oscillatory physiological waveform and (b) parabolic inlet velocity profile; (c) pressure distribution in 65% stenotic artery from different mesh sizes.

IV. Numerical Scheme

The numerical simulations are performed by well-known software ANSYS Fluent 16. A pressure based algorithm is chosen as the solver type. This solver is generally selected for an incompressible fluid. As there is no heat transfer in the blood flow process, energy equation is not solved. Since turbulent is expected in 85% stenotic artery at post stenotic region, a low Reynolds number $k-\omega$ turbulent model is used throughout the work. In solution methods, the SIMPLE algorithm is selected for pressure-velocity coupling. First Order Upwind scheme is employed as a numerical scheme for discretization of the momentum equation. The time step is set to 0.00041 sec with 2000 number of total time steps. Maximum 10 iterations are performed per each time step.

V. Validation

Validation of the present numerical computation has been done by plotting the steady velocity profile at 2.5D downstream from the stenosis throat and comparing it with the velocity profile of Varghese and Frankel [27]. For this case, a parabolic velocity profile has been assumed as inlet boundary condition. The mean inlet velocity corresponds to Reynolds number 500 and the flow has been assumed to be steady. The results have been shown in the Figure 4, where a good agreement can be found with Varghese and Frankel [27].

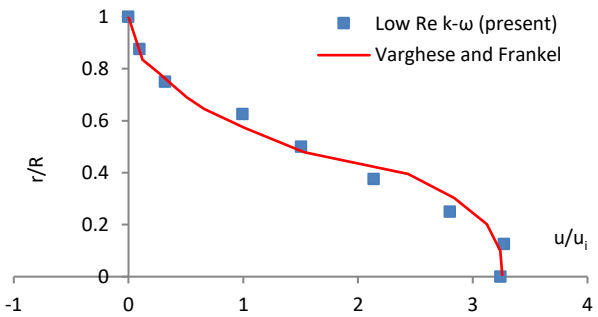

Fig 4: Validation with the velocity profile of Varghese and Frankel [27].

VI. Results and Discussion

The computational results are taken to study the influence of stenosis and bifurcation on the flow behavior. Actually, transient or unstable flow separation that creates flow disturbance regions is associated with a predisposition to atherosclerosis at branches, bifurcations and curvatures in the arterial circulation. Thus the flow parameters are observed from the contours at specific instants of pulse cycle.

To strengthen the logic of using low Reynolds number k-w turbulence model in the calculation, the numerical results by the low Re-number k-w model were compared with the results by the laminar model in terms of velocity and wall shear stress. Figures 5 and 6 have shown that the velocity and wall shear stress profiles by the low Re-number k-w model are in good agreement with the results by the laminar model. However, some little discrepancies are found in the results of velocity and wall shear stress distribution at early diastole due to disturbed flow. Therefore, there is no barrier to use low Reynolds number k-w turbulence model for the calculation.

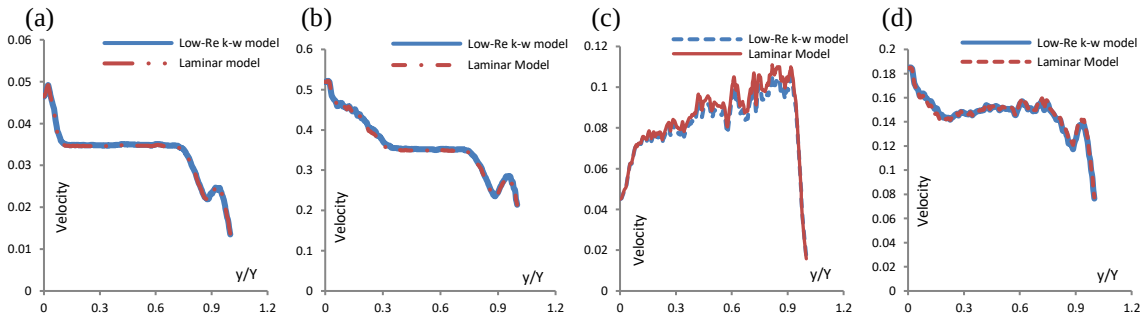

Fig. 5: Comparison of the velocity by the low-Re k-w model with the laminar model at (a) early systole, (b) peak systole, (c) early diastole and (d) diastole for the Healthy Carotid Artery.

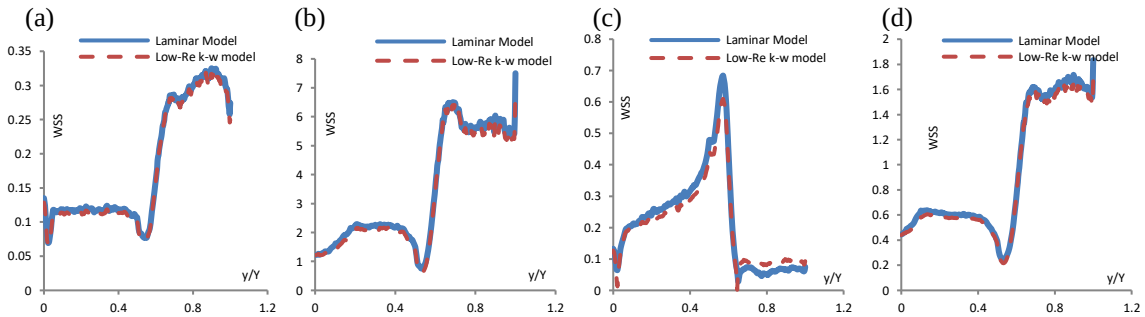

Fig. 6: Comparison of the Wall Shear Stress by the low-Re k-w model with the laminar model at (a) early systole, (b) peak systole, (c) early diastole and (d) diastole for the Healthy Carotid Artery.

The interaction between hemodynamic and the endothelium is an important determinant of cardiovascular function. Actually, Wall Shear Stress is very essential factor for understanding the severity level of arterial diseases. Endothelium lining the circulatory system is highly sensitive to hemodynamic shear stresses that act at the vessel surface in the direction of blood flow. A prolonged high wall shear stress fragments the internal elastic lamina of vessels and gives rise to the initial change involved in the formation of an atherosclerosis or an aneurysm. Actually, it is a flow-induced stress that can be described as the frictional force of viscous blood. Besides, it is the force per unit area created when a tangential force due to blood flow acts on the vessel's surface (endothelium). Thus, it acts directly on the vascular endothelium as a biological stimulator that modulates the cellular function of the endothelium. However, it can be determined by the mean fluid flow rate, its viscosity, and the physical dimensions of blood vessels. For Poiseuille flow, shear stress (τ) is directly proportional to the velocity of blood flow, and inversely proportional to the cube of the arterial radius (R), where Q is flow rate and $\mu$is fluid viscosity. Then, $\tau = 4\mu Q/R^3$. Thus, small changes in R greatly influenceτ, and vice versa.

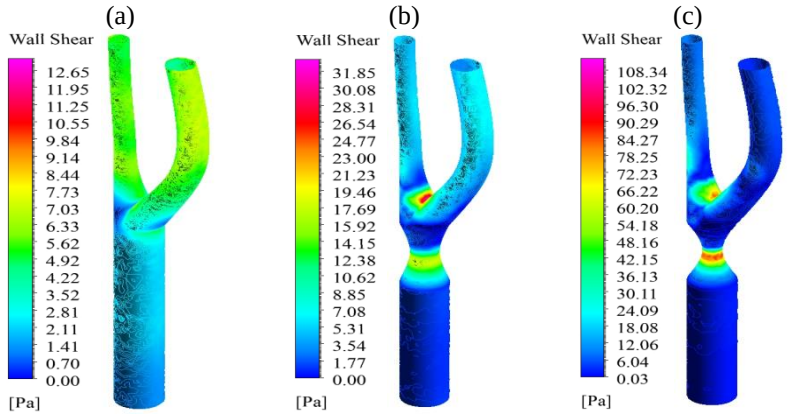

Fig. 7: Wall Shear Stress Distributions in (a) healthy Carotid artery, (b) 65% stenotic Carotid artery and (c) 85% stenotic Carotid artery at peak systole.

In the arterial circulation, WSS has a vital role in determining where most vascular pathology originates [28]. Moreover, it is responsible for the development of endothelial phenotypic changes in which the metabolic balance is disrupted that are associated with the initiation and development of the atherosclerosis [29, 30]. High WSS elongates the endothelial cells and force to align in the direction of the flow. On the other hand, low WSS had negligible effect on the cell but increases intercellular permeability and consequently increases the plaque formation in the region. Thus, endothelial cells react differently to the high and low WSS. Consequently, WSS is mostly responsible for creating a new stenosis throat. Moreover, the proximity of high and low WSS in a small aneurysm region might enhance the degenerative change of the aneurysm wall.

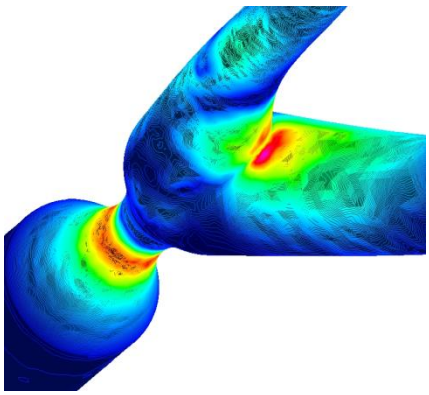

Fig. 8: Wall Shear Stress Distribution at the throat and bifurcation region of 85% stenotic Carotid artery at peak systole.

Figure 7 shows the distributions of Wall Shear Stress in healthy, 65% and 85% stenotic Carotid arteries at peak systole. No significant variation in WSS has been seen in healthy carotid artery. The highest WSS of the healthy artery is approximately 13 Pa. However, remarkable changes in WSS are noticed at throat and bifurcation regions of the stenotic carotid arteries. Besides, the highest WSS of the 65% and 85% stenotic arteries are about 32 Pa and 113 respectively. The WSS has increased abnormally at the 85% stenotic Carotid artery. From the figure 8, it is clear that bifurcation area of 85% stenotic carotid artery generates the highest WSS, so bifurcation region is the most risky area of the carotid artery.

Variations of streamlines contours have been investigated for healthy and stenotic carotid arteries to study the flow pattern of blood through the arteries. Streamline distribution for the models at peak-systole is shown in figure 9. There is no recirculation region in the healthy artery and streamlines run smoothly throughout the geometries. However, a very small recirculation region is noticed after the throat and near the bifurcation area of 65% stenotic carotid artery, except this most of the streamlines run smoothly throughout the geometry. A long disturbed flow has been found in 85% stenotic carotid artery. The recirculation region has started at the throat and continued to be disturbed at the internal and external carotid arteries. The stenotic jets have been appeared in the stenotic carotid arteries due to the constriction of the arteries. From figure 2 it has been noticed that Reynolds number rose abnormally at peak systole at throat region of 85% stenotic carotid artery. Thus, it

was expectable that the flow might be disturbed at peak systole in the 85% stenotic carotid artery. However, at early diastole the Reynolds number is very low. Thus, flow should be smooth, but from figure 10 it has been found that the flow is very disturbed in all models and the recirculation region is appeared even in the healthy artery. How is it possible without any constriction of artery and with very low Reynolds number? Thus, steady flow has been investigated in the healthy artery remaining all the condition same as like as unsteady flow at early diastole. The result has been shown in the figure 11 and it has been noticed that there is no recirculation region and the flow is very smooth. Therefore, it can be said that transient or unstable flow can create flow disturbance regions in the arteries.

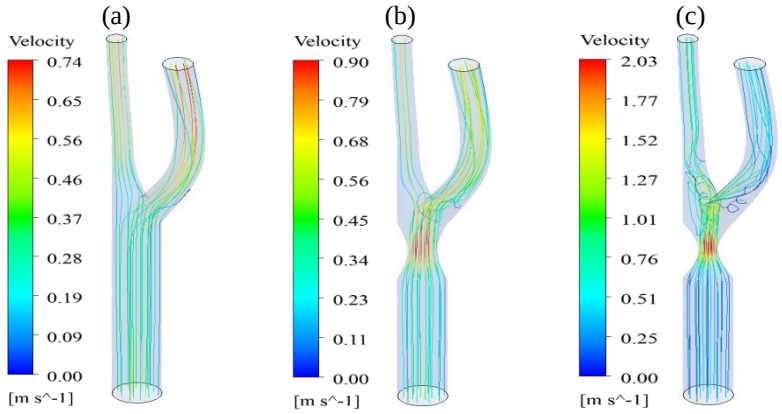

Fig. 9: Streamlines Distributions in (a) healthy Carotid artery, (b) 65% stenotic Carotid artery and (c) 85% stenotic Carotid artery at peak systole.

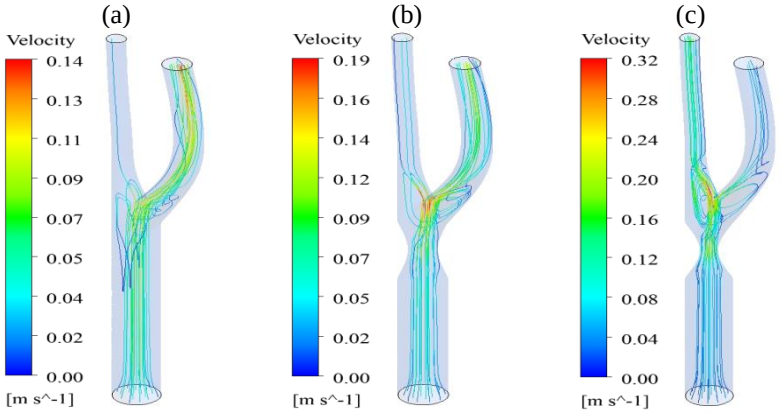

Fig. 10: Streamlines Distributions in (a) healthy Carotid artery, (b) 65% stenotic Carotid artery and (c) 85% stenotic Carotid artery at early diastole.

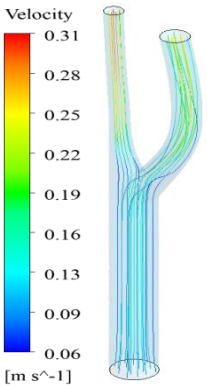

Fig. 11: Streamlines Distributions for steady flow in healthy Carotid artery.

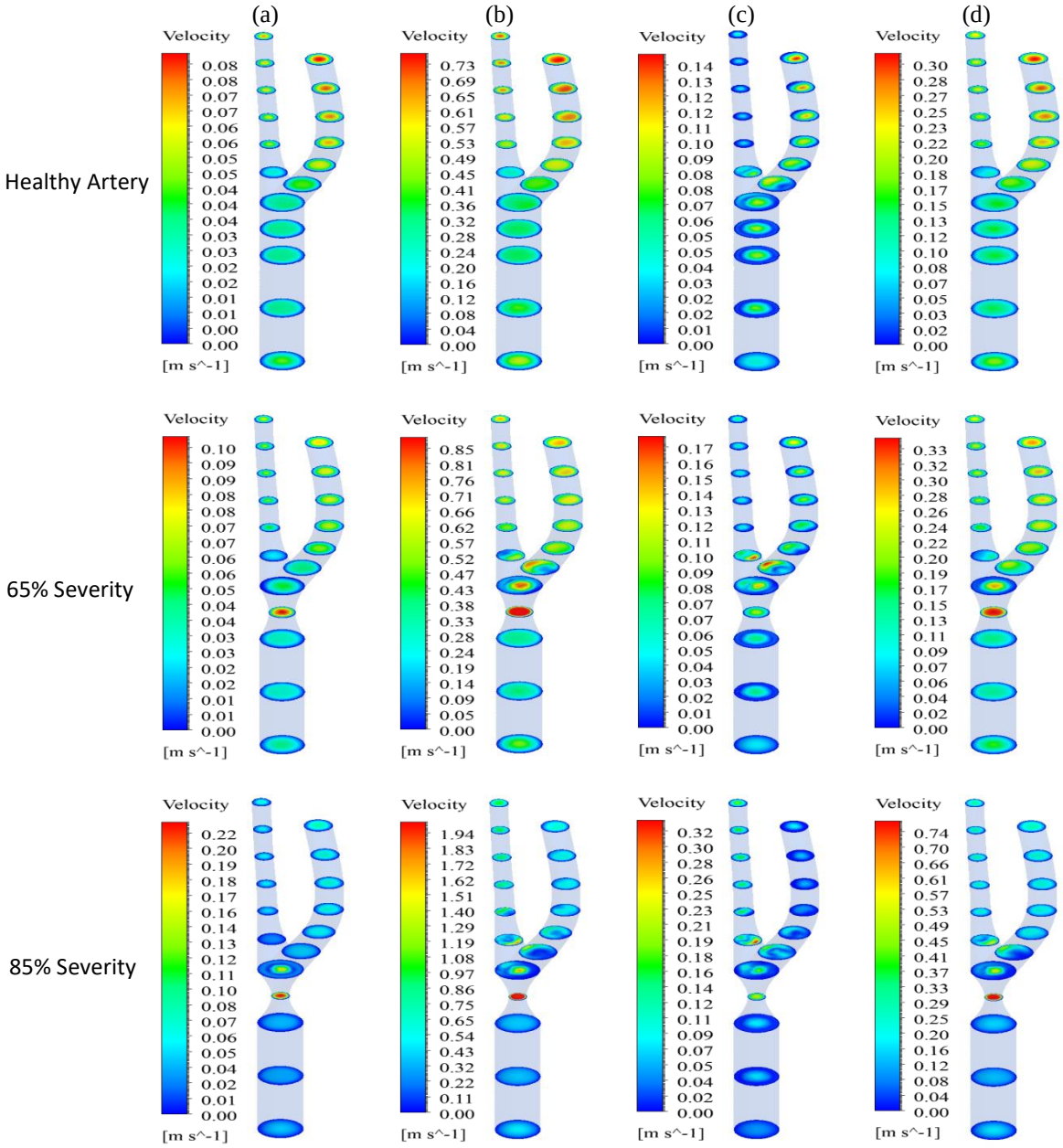

Fig. 12: Axial velocity on different axial slices of Carotid Artery with different severities at (a) early systole, (b) peak systole, (c) early diastole and (d) diastole.

The figure 12 provides the contour distribution of the axial velocity on different axial slices of carotid arteries at four time instants such as early systole, peak systole, early diastole and diastole. This figure exhibits the flow disturbances in the carotid arteries. As is observed, the flow has been disturbed in 85% stenotic carotid artery at most of the cardiac cycle. According to the figure, in healthy artery there is no disturbed flow at the whole cardiac cycle except the early diastole. The reason behind this, which has already been described, is unsteady flow condition. Meanwhile, a moderate disturbed flow has been seen in the 65% stenotic carotid artery at the whole cardiac cycle except the early systole. Moreover, a similar pattern but more severe disturbance in the flow is observed in the 85% stenotic carotid artery. In brief, disturbance of flow has risen as the severity of stenosis in the artery has been increased.

VII. Conclusion

Numerical simulation has been done on physiological blood flow through carotid arteries with different severities of stenosis. From the investigation it is concluded that the low-Re k-w turbulence model can provide satisfactory information regarding blood flow in arterial stenoses, which is difficult to obtain accurately by experimental methods. Furthermore, bifurcation area is the most risky region of carotid artery because highest wall shear stress is observed there. Another observation is that transient or unstable flow can create flow disturbance regions in the arteries. Moreover, the disturbance of flow has risen as the severity of stenosis in the artery has been increased.

Nomenclature:

D	Diameter of the healthy artery	x	Axial location of the flow field
L	Length of the artery	g	Acceleration due to gravity
r	Radial location of the flow field	t	Time period of the inlet flow cycle
R	Radius of the healthy artery	u	Instantaneous velocity
U	Average velocity	WSS	Wall shear stress
μ	Constant viscosity of blood	ρ	Density of blood
LDL	Lower density Lipoprotein	3D	Three Dimension
PDE	Partial Differential Equation	Re	Reynolds Number
τ	Shearing stress	ν	Kinematic viscosity of the fluid
γ	Shear rate	k	Turbulent kinetic energy
ε	Dissipation of turbulent kinetic energy	UDF	User Defined Function

Reference

[1] Smith, F. T. The separation flow through a severely constricted symmetric tube. Journal of Fluid Mechanics, 90: 725-754, 1979

[2] Deshpande, M. D., Geidens, D. P. and Mabon F. R. Steady laminar flow through modelled vascular stenoses. Journal of Biomechanics, 9: 165-174, 1976

[3] Young, D. F. and Tsai, F. Y. Flow characteristics in models of arterial stenosis: I steady flow. Journal of Biomechanics, 6: 395-410, 1973

[4] Imaeda, K. and Goodman, F. O. Analysis of nonlinear pulsatile blood flow in arteries. Journal of Biomechanics, 13: 165-174, 1980

[5] Misra, J. C. and Chakravaty, S. Flow in arteries in the presence of stenosis. Journal of Biomechanics, 19: 907-918, 1986

[6] Young, D. F. and Tsai, F. Y. Flow characteristics in models of arterial stenosis: II unsteady flow. Journal of Biomechanics, 6: 547-559, 1973.

[7] S. Khader and B. Shenoy., "Effect of increased severity in patient specific stenosis, World journal of Modelling and Simulation", Vol. 7 No. 2, pp. 113-122, (2011).

[8] C, Chua and G. Shread., "Changes in flow and wall stresses through arterial constriction offset from the centre of the vessel", The Anziam Journal, 50: C744-C759, (2009).

[9] V. Young, A. Patterson M. Graves, Z-Y LI, V. Tavani, T. Tang, and J. H. Gillard, The mechanical triggers of rupture: shear vs pressure gradient, The British J. of Radiology, 82 (2009) S39-S45

[10] Stroud, J. S. A. Berger and D. Saloner., "Numerical analysis of flow through a severely stenotic carotid artery bifurcation", J. Biomech. Eng.124:9-20, (2002).

[11] Boughner DR, Roach MR. "Effect of low frequency vibration on the arterial wall" Circ. Res., 1971; 29:136–144.

[12] Cassanova RA, Giddens DP. "Disorder distal to modeled stenoses in steady and pulsatile flow" J. Biomech., 1978; 11:441–453.

[13] Roach MR. "Poststenotic dilatation in arteries" Cardiovascular Fluid Dynamics, 1972; 2:111–139.

[14] Giddens DP, Mabon RF, Cassanova RA. "Measurements of disordered flows distal to subtotal vascular stenoses in the thoracic aortas of dogs" Circ. Res., 1976; 39:112–119.

[15] Clark C. "Turbulent velocity measurements in a model of aortic stenosis" J. Biomech., 1976; 9:677–687.

[16] Strandness DE JR., Didisheim P, Clowes AW, Watson JT., Eds. ''Vascular Disease–Current Research and Clinical Applications" Orlando, USA: Grune and Stratton; 1987.

[17] Yongchareon W, Young DF. Initiation of turbulence in models of arterial stenoses. J. Biomech., 1979; 12:185–196.

[18] Jones SA. A study of flow downstream of a constriction in a cylindrical tube at low Reynolds numbers with emphasis on frequency correlations. Ph.D. Thesis, University of California; 1985.

[19] M. G. Rabby, A. Razzak, and Md. M. Molla, Pulsatile non-Newtonian blood flow through a model of arterial stenosis; Procedia Engineering 56 (2013) 225-231.

[20] Pedley, T. J. The Fluid Mechanics of Large Blood Vessels. Cambridge University Press, 1980

[21] Berger, S. A. and Jou, L. –D. Flow in stenotic vessels. Annual Reviews of Fluid Mechanics, 32:347-382, 2000

[22] Chien, S., 1981 Hemorheology in clinical medicine, Recent advances in Cardiovascular Diseases 2 (Suppl.), p.21.

[23] K. Mamun, M.N. Akhter, M.S.H. Mollah, M.A.N. Sheikh, and M. Ali, Characteristics of pulsatile blood flow through 3-D geometry of arterial stenosis, Procedia Engineering 150 (20015) 877-884.

[24] Wilcox DC. "Turbulence Modeling in CFD" La Canada California: DCW Industries; 1993.

[25] M. M. Cross, Journal of Colloid Science, 20, 417–437 (1965).

[26] K. Mamun, M.M. Rahman, M.N. Akhter and M. Ali, Physiological non-Newtonian blood flow through single stenosed artery, AIP Conference Proceedings 1754, 040001 (2016); doi: 10.1063/1.4958361

[27] S.S. Varghese and S.H. Frankel, Numerical Modeling of Pulsatile Turbulent Flow in Stenotic Vessels, J. Biomech, Vol. 125, pp. 445-460, 2003.

[28] Glagov S, et al. Hemodynamics and atherosclerosis. Insights and perspectives gained from studies of human arteries. Arch Pathol Lab Med 1988; 112:1018–1031. [PubMed: 3052352]
[29] Passerini AG, et al. Coexisting proinflammatory and antioxidative endothelial transcription profiles in a disturbed flow region of the adult porcine aorta. Proc Natl Acad Sci USA 2004; 101:2482–2487. [PubMed: 14983035]
[30] Volger OL, et al. Distinctive expression of chemokines and transforming growth factor-beta signaling in human arterial endothelium during atherosclerosis. Am J Pathol 2007; 171:326–337. [PubMed: 17591977]

Khairuzzaman Mamun "Simulation of Physiological Non-Newtonian Blood Flow through 3-D Geometry of Carotid Artery with Stenosis." IOSR Journal of Mechanical and Civil Engineering (IOSR-JMCE), vol. 15, no. 1, 2018, pp. 33-43